Neutron scattering studies of the vibrational spectrum of high-density amorphous ice in comparison with ice Ih and VI

1994 J. Phys.: Condens. Matter 6 375

(http://iopscience.iop.org/0953-8984/6/2/009)

J. Phys.: Condens. Matter 6 (1994) 375–382. Printed in the UK

Neutron scattering studies of the vibrational spectrum of high-density amorphous ice in comparison with ice Ih and VI

A I Kolesnikov†, V V Sinitsyn†, E G Ponyatovsky†, I Natkaniec‡ and L S Smirnov‡

† Institute of Solid State Physics, Russian Academy of Sciences, 142432 Chernogolovka, Moscow District, Russia

‡ Frank Laboratory of Neutron Physics, Joint Institute for Nuclear Research, 141980 Dubna, Moscow District, Russia

Received 6 September 1993

Abstract. The vibrational spectrum of recovered high-density amorphous (HDA) ice, obtained by pressurizing hexagonal ice Ih to 13 kbar at 77 K, has been studied by inelastic incoherent neutron scattering in the energy range from 1 to 120 meV at 80 K. The spectra of ice Ih and recovered high-pressure phase ice VI were also measured for comparison. In the translational band of the HDA ice spectrum, the first peak in the acoustic mode region is shifted by 2 meV towards high energies, but in the librational band the spectrum shows that the low-energy cut-off of this band shifts 13 meV towards low-energy transfers compared with ice Ih. Similarity of the main features of the spectra of HDA ice and ice VI have been observed and, thus, the dynamics of these ice phases should be determined by the same atomic correlations and force constants.

1. Introduction

Recently a number of neutron diffraction and inelastic incoherent neutron scattering (INS) experiments have been applied to study the structure and dynamics of various phases of ice. One of the most interesting results of these investigations was the observation of the transition of ice to a high-density amorphous (HDA) phase. Usually the HDA ice is produced by pressurizing hexagonal ice Ih to 10 kbar at 77 K [1], and this phase can be recovered at an ambient pressure (the density of the recovered HDA ice at 77 K is 1.17 g cm^{-3} at zero pressure). This transformation was interpreted in [1] as the melting of ice at a low temperature, because the melting line of ice Ih when extrapolated to 77 K lies below 10 kbar. Recently, molecular dynamics calculations have been applied to the study of the stress-induced crystalline-to-amorphous transformation in ice [2, 3]. A careful analysis of the dynamics of the transformation showed that the mechanism is a collapse of the hexagonal framework of water molecules and a gradual filling of the voids in the lattice under the application of pressure.

Another way of producing HDA ice was proposed in [4]. The high-pressure phase ice VIII has 'melting' curves with a positive slope, and it was suggested that ice VIII recovered at 77 K might convert to HDA ice after heating it carefully. This transformation was successfully realized in [5], where the transitions at heating of the recovered ice VIII to HDA and low-density amorphous (LDA) ices, and then to cubic ice Ic and Ih were observed by real-time neutron diffraction.

In the pressure range from 2 to 25 kbar there are at least eight phases of ice (ice II–IX). Some of these can be recovered by cooling to liquid-nitrogen temperature before releasing

0953-8984/94/020375+08$07.50

the pressure. Because of this property the structures and vibrational spectra of most of the high-pressure polymorphous ices have been studied. The density of ice increases as the formation pressure increases, and an increase in the nearest neighbour distances O–H...O was revealed. The increase in the density of ices may be regarded as arising from increased efficiency of molecular packing of neighbours. The O–O–O interbond angles in these phases change so that they become closer to the exact tetrahedral value. Moreover, for the phases formed under a pressure greater than 10 kbar (ices VI, VII and VIII) a qualitative structure reconstruction takes place. Their structure can be described as made up from two interpenetrating sublattices. Each of these sublattices is hydrogen bonded within itself, but they are not hydrogen bonded to each other. This kind of structural arrangement has been called 'self-clathrate'.

The structural differences in ice phases lead to common conformity in the transformation of their phonon spectra. The spectra in the translational region show that the first peak in the acoustic mode region is shifted towards a higher energy, while the whole librational band is shifted to a lower energy, as the phase formation pressure increases [6–8] (except for ice VIII, in which no further shifts towards lower energies were observed [9] compared with ice VI, although the formation pressure increases). This shift in the librational band can be explained mainly by the reductions in the O–H...O bending force constant.

Up to now the vibrational spectrum of HDA ice has been studied by the IINS technique only in [10], where the spectrum of HDA ice has been analysed with reference to the spectra of the low-density ices Ih and Ic and LDA ice. Their results show that the librational band in the HDA ice spectrum is shifted towards a lower energy as mentioned above, but the first peaks in the acoustic mode region were very similar for all four phases. The invariability of this peak for ice phases with low and high densities disagrees with the analogous IINS measurements for other phases of ice. Thus, the dynamics of this singular case for HDA ice, which is outside the 'family' of all the other ices, should be clarified.

Here we report the results of an IINS investigation of vibrational spectrum of HDA ice in the range of translational and librational bands (0–150 meV). The data obtained are compared with the spectra of ice Ih and the recovered high-pressure phase ice VI (the latter was measured exactly at the same conditions as for the HDA ice). The data obtained undoubtedly show that main features of the IINS spectrum for HDA ice are similar to those of the spectrum for ice VI.

2. Experimental details and data treatment

The material used in the sample preparation was doubly distilled H_2O. The high-pressure ice phases were prepared at the Institute of Solid State Physics. The ice VI was produced in toroid-type chamber applying a pressure of 15 kbar at room temperature, cooling the chamber to about 100 K and releasing the pressure at that temperature. The HDA ice was prepared using a piston-and-cylinder high-pressure chamber, which can be disassembled in liquid nitrogen. The crystalline ice Ih was cooled to about 77 K at atmospheric pressure, compressed to 15 kbar and kept for $\frac{1}{2}$ h under these conditions; and then the pressure was released at the same temperature. An abrupt decrease in sample volume was observed at about 12.5 kbar during the continuous process of increasing the pressure (friction was not taken into account). According to [11], this indicated a transformation from Ih to HDA ice.

The samples of recovered HDA ice and VI ice (each of mass about 0.5 g) were powdered under liquid nitrogen, packed into a flat aluminium container and stored in liquid nitrogen. The samples in the container were then mounted into a top loading cryostat with aluminium windows, and experiments were performed at 80 K.

The IINS measurements were carried out in neutron energy loss mode using an inverted geometry time-of-flight KDSOG-M spectrometer for the HDA ice and VI ice and a NERA-PR spectrometer for the ice Ih (of mass about 5 g) installed at the IBR-2 pulse reactor in Dubna [12]. The incident neutron energy is determined by the reactor–sample flight path (29.7 m for the KDSOG-M spectrometer and 109.1 m for the NERA-PR spectrometer) and the energy of scattered neutrons by the pyrolitic graphite analysers ($E_f = 4.7$ meV), mounted behind a beryllium filter at 80 K. The spectrometers provided medium resolution for the KDSOG-M spectrometer, $\Delta\omega/\omega \simeq 4$–8% and excellent resolution for the NERA-PR spectrometer, $\Delta\omega/\omega \simeq 2$–3%, in the range of energy transfer studied from 1 to 120 meV. Because of the small amount of the recovered high-pressure phases of ice the experiments with these samples were carried out on the KDSOG-M spectrometer with a high neutron flux at the sample position compared with the NERA-PR spectrometer.

The estimated neutron transmission through the samples exceeded 80% and multiple-scattering contributions were not taken into account. After subtraction of the background determined in separate empty-can measurements under the same conditions as for the samples, the data were transformed to the generalized vibrational density of states (GVDS) $G(\omega)$ versus energy transfer (in millielectronvolts) using standard programs.

The contributions from the multiphonon neutron scattering (up to four-phonon processes) were calculated in a harmonic isotropic approximation by the multiconvolution of the one-phonon spectrum using an iterative technique [13–15]. Experimental data in the energy range of the translational and librational bands, 1–120 meV, were used at the first iterative step as the one-phonon spectrum. In the second and subsequent steps, the one-phonon spectrum was assumed to be the difference between the experimental spectrum and that resulting from the multiphonon processes. For all measured spectra the convergence was reached in three iterations.

3. Results and discussion

Figure 1 shows the measured $G(\omega)$ spectra (full circles) and calculated one-phonon (full curves) and multiphonon (broken curves) neutron scattering contributions for the HDA ice, ice IV and ice Ih. The spectra consist of two bands: the lower 0–40 meV band associated with translational vibrations of the water molecules, and the upper 50–120 meV band which is due to their librations. The contribution of multiphonon processes in the range of the translational part, about 15–20% of the total intensity, are smooth and flat, but in the range of the librational bands the multiphonon scattering looks like a smooth hill which is almost unstructured. Note that their intensity exceeds the one-phonon contribution at high energies and is about 48, 55 and 76% of the total intensity for ice VI, HDA ice and ice Ih, respectively. The greater multiphonon contribution for ice Ih is due to its much softer acoustic part, where the phonon population increases with decreasing energy. The shape and intensity of the spectra in the energy range $\omega > 120$ meV are well described by contributions from the multiphonon neutron processes.

We briefly compare the data obtained for crystalline ice phases with those measured recently on the TFXA spectrometer at the ISIS neutron source [6, 8], and all the assignments of the spectral peculiarities should be referred to these papers. Note that the $G(\omega)$ spectrum for ice Ih (see figures 1 and 2) measured with high resolution on the NERA-PR spectrometer exhibits features (even a fine structure) qualitatively and quantitatively which are very similar to those observed in [6, 8]. The first peak in the acoustic mode region has a maximum at 7 meV, a sharp bend at 9 meV and a shoulder at 13 meV. The width of this acoustic band

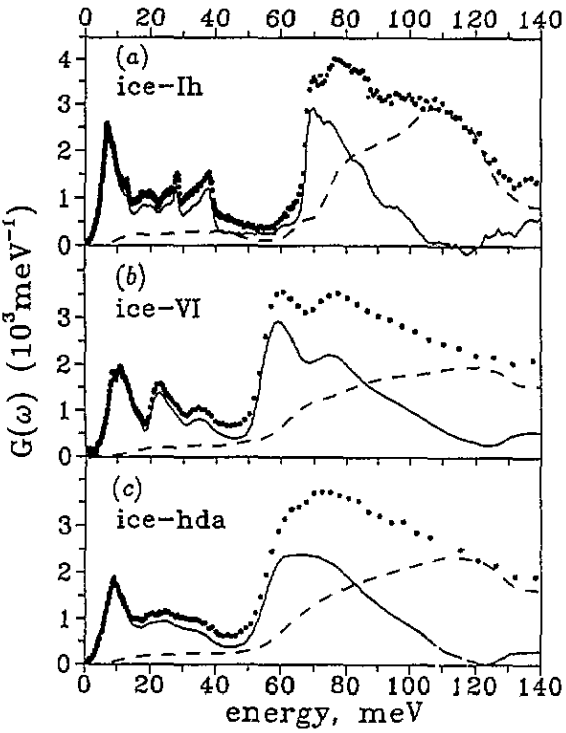

Figure 1. Plots of the GVDOS $G(\omega)$ for (*a*) the H_2O ice Ih and the recovered high-pressure phase of (*b*) ice VI and (*c*) HDA ice: ●, experimental total spectra; – – –, calculated multiphonon neutron scattering contributions; ——, one-phonon spectra.

at half-maximum is 6.5 meV for the measured $G(\omega)$ and somewhat narrower, 5.9 meV, for the extracted one-phonon spectrum. The latter value differs slightly from the value of 7.9 meV measured in [6] but is in exact accord with the width in the calculated $G(\omega)$ spectrum for ice Ih in [16]. For a higher energy of the translational region a broad flat hump is seen at around 19 meV, a sharp peak at 28 meV and a triangular peak with a maximum at 37.5 meV. The high-energy cut-off of the translational band occurs at 40 meV.

The librational band of ice Ih exhibits a sharp low-energy cut-off at about 66.5 meV. The structure of the band in the measured $G(\omega)$ has two subbands and a minimum at about 90 meV. It follows from the multiphonon calculations that the right-hand subband originates mainly from the multiphonon neutron scattering, and the high-energy side of the one-phonon librational band is gently sloping and edged at 105 meV. These data disagree with results of the measurements on the HET spectrometer [7] which provides a smaller value of the neutron momentum transfer and hence a decrease in the multiphonon contribution. However, the librational band calculated in [17, 18] looks very similar to our one-phonon spectrum, which assures us that the data obtained are close to reality.

In the case of ice VI, the spectrum measured on the KDSOG-M spectrometer with medium resolution is very similar to the results in [6]. For the acoustic modes (figures 1 and 2), the first peak is split into two lines at 9 and 11 meV, in agreement with [6], but a similar splitting does not appear for the other modes at 23 and 35 meV, which were split in the ice VI spectra measured on the TFXA spectrometer [6] with better resolution. The low-energy edge of the librational band (figures 1 and 3) is shifted towards a lower

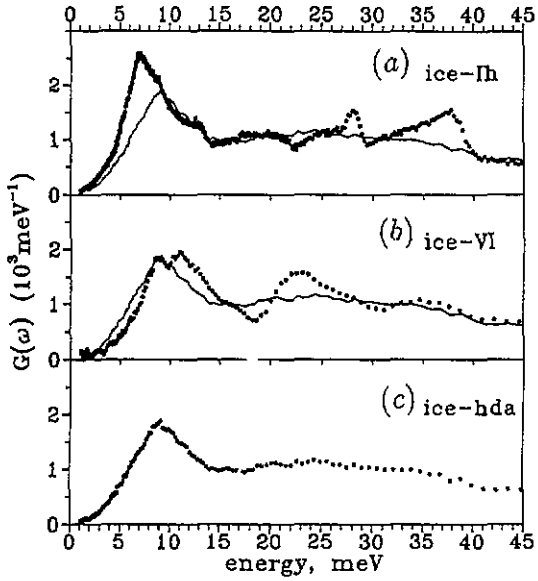

Figure 2. The GVDSs (●) for (*a*) H_2O ice **Ih**, (*b*) ice VI and (*c*) HDA ice in the energy range of the translational band: ——, spectrum of the HDA ice in (*a*) and (*b*) for better visual comparison.

energy compared with ice Ih by about 13 meV. The structure of the band for ice VI has two maxima, at 61 meV and 77.5 meV (59.5 meV and 75.5 meV respectively, for the one-phonon spectrum), and the high-energy cut-off of the one-phonon spectrum is at about 120 meV.

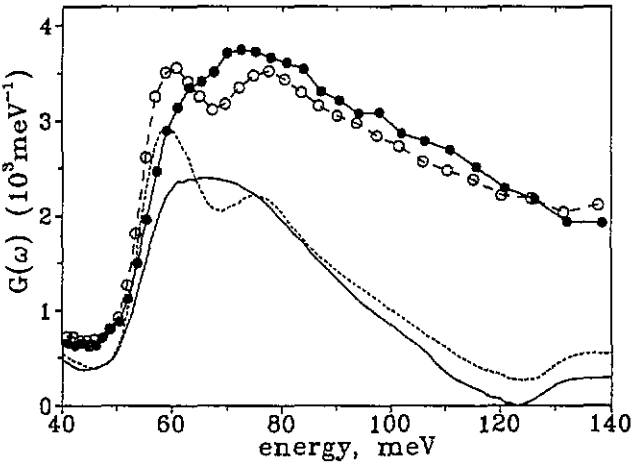

Figure 3. The GVDSs for H_2O ice VI (○) and HDA ice (●) in the energy range of the librational band: ----, one-phonon spectrum of ice VI; ——, one-phonon spectrum HDA ice.

The first peak in the acoustic region of the translational band of the HDA ice spectrum has a maximum at 9 meV. For other ice phases the maxima of this peak appear at energy values of about 7 meV for Ih, 8.7 meV for ice V, 9 and 11 meV for ice VI, about 9 meV

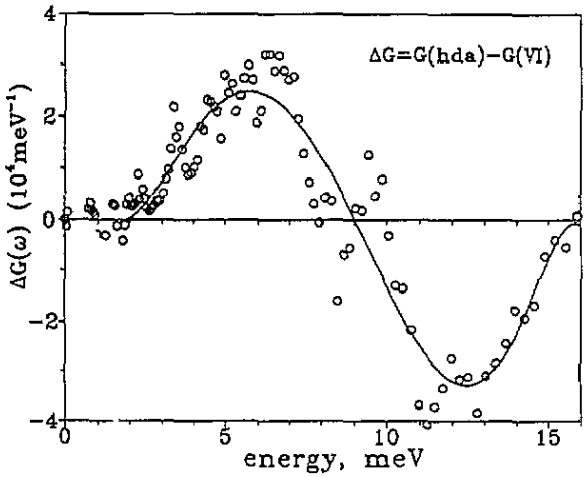

Figure 4. Difference (○) between the GVDSs for HDA ice and ice VI in the acoustic mode region: ——, curve obtained by fitting the polynomial to the data points.

for ice IX, around 10 meV for ice II, and 14.7 meV for ice VIII (see [6, 8, 9] and the present data). In order to make the comparison between the measured HDA ice spectrum and those for the crystalline Ih and VI more visual in the region of the acoustic modes, each of them is shown in figure 2 with superposition of the HDA ice spectrum (full curves). Figure 2 clearly shows the hardening of the first peak in the acoustic region for HDA ice compared with ice Ih. This provides the common rule of conformity in the transformation of ice vibrational spectra depending on the phase formation pressure, which is mentioned in the introduction.

The low-energy cut-off of the librational band in the spectrum of HDA ice shifts to lower-energy transfers by approximately 13 meV for ice Ih, 9 meV for ice IX, and 4 meV for ice II and ice V, and it exactly coincides with that for ice VI and ice VIII [6–9].

The structure of $G(\omega)$ for HDA ice, especially in the range of the librational band at 50–120 meV and around the first acoustic peak at 9 meV, resembles much more that of ice VI than that of the other ice phases. This indicates the existence of the same mean atomic correlations and force constants, which determine the dynamics of these ice phases. Similar to the self-clathrate structure of ice VI, which can be described as made up from two interpenetrating sublattices, the structure for HDA ice also must consist of two interpenetrating hydrogen-bonded networks, but they are not hydrogen bonded to each other.

The essential difference between the two spectra is a smooth structure of the translational and librational bands for HDA ice. We interpret this difference as being due to defects in the HDA ice in essentially the same basic building units as for ice VI, which leads to a slight change in the short-range order, and to a complete loss of the long-range order.

At energy transfers below 9 meV, there is a clear difference between the spectra of HDA ice and ice VI. The left-hand slope of the peak for HDA ice became more intensive, owing to the presence of the low-energy modes (LEMs) as the result of amorphization. Figure 4 shows the difference between the GVDSs of the HDA ice and ice VI, and the peak at around 6 meV can be assigned to LEMs. The presence of LEMs in the GVDS of disordered solids, e.g. glasses, is normal [19]; they play an important role in the dynamics of amorphous systems. We attribute the LEMs observed in the GVDS of the HDA ice to a strong disorder in the molecular short-range order. Also, the metastability of the sample itself could lead to a large softening of the vibrational spectrum [20, 21].

It was shown recently by neutron diffraction that the pair correlation function of the HDA ice is very similar to that of liquid water at a high temperature (90 °C) [22] or liquid water at a high pressure (10 kbar) [23]. Thus, we can suppose that the structure of liquid water at a high pressure or a high temperature consists of some clusters with the short-range order being similar to that of ice VI.

4. Conclusions

The GVDSs of HDA ice and ice VI show the same main structure: the acoustic peak maximum at 9 meV and the same low- and high-energy edges of the librational band. We, therefore, conclude that essentially the same atomic correlations and force constants determine the dynamics of these ice phases. The structure for HDA ice must consist of two interpenetrating hydrogen-bonded networks, but they are not hydrogen bonded to each other. In analogy to ice VI, ice VII and ice VIII, the structure of the HDA ice can be called 'self-clathrate'.

Acknowledgment

We would like to thank A Muzychka for technical assistance.

References

[1] Mishima O, Calvert L D and Whalley E 1984 *Nature* **310** 393–5
[2] Tse J S 1992 *Physics and Chemistry of Ice* ed N Maeno and T Hondoh (Sapporo: Hokkaido University Press) pp 91–7
[3] Tse J S 1992 *J. Chem Phys.* **96** 5482–7
[4] Klug D D, Handa Y P, Tse J S and Whalley E 1989 *J. Chem. Phys.* **90** 2390–2
[5] Balagurov A M, Barkalov O I, Kolesnikov A I, Mironova G M, Ponyatovskii E G, Sinitsyn V V and Fedotov V K 1991 *JETP Lett.* **53** 30–3
[6] Li J-C, Londono J D, Ross D K, Finney J L, Tomkinson J and Sherman W F 1991 *J. Chem. Phys.* **94** 6770–5
[7] Li J-C, Londono J D, Ross D K, Finney J L, Bennington S M and Taylor A D 1992 *J. Phys.: Condens. Matter* **4** 2109–16
[8] Li J-C, Ross D K, Londono J D, Finney J L, Kolesnikov A and Ponyatovskii E G 1992 *Physics and Chemistry of Ice* ed N Maeno and T Hondoh (Sapporo: Hokkaido University Press) pp 43–9
[9] Kolesnikov A I, Li J-C, Ross D K, Sinitzin V V, Barkalov O I, Bokhenkov E L and Ponyatovsky E G 1992 *Phys. Lett.* **168A** 308–12
[10] Klug D D, Whalley E, Svensson E C, Root J H and Sears V F 1991 *Phys. Rev.* B **44** 841–4
[11] Floriano M A, Handa Y P, Klug D D and Whalley E 1989 *J. Chem. Phys.* **91** 7187–92
[12] Belushkin A V (ed) 1991 *User Guide, Neutron Experimental Facilities at JINR* (Dubna: Joint Institute for Nuclear Research) p 72
[13] Antonov V E, Belash I T, Kolesnikov A I, Mayer J, Natkaniec I, Ponyatovsky E G and Fedotov V K 1991 *Sov. Phys.–Solid State* **33** 87–90
[14] Kolesnikov A I, Prager M, Tomkinson J, Bashkin I O, Malyshev V Yu and Ponyatovskii E G 1991 *J. Phys.: Condens. Matter* **3** 5927–36
[15] Kolesnikov A I, Natkaniec I, Antonov V E, Belash I T, Fedotov V K, Krawczyk J, Mayer J and Ponyatovsky E G 1991 *Physica* B **174** 257–61
[16] Li J-C and Ross D K 1992 *Physics and Chemistry of Ice* ed N Maeno and T Hondoh (Sapporo: Hokkaido University Press) pp 35–42
[17] Tse J S, Klein M L and McDonald I R 1983 *J. Phys. Chem.* **87** 4198–203
[18] Belosludov V R, Lavrentiev M Yu, Syskin S A and Dyadin Yu A 1987 *Preprint* Institute of Inorganic Chemistry USSR Academy of Sciences, Siberian Branch, Novosibirsk, USSR, 87-4 p 42 (in Russian)
[19] Suck J-B and Rudin H 1983 *Glassy Metals II (Topics in Applied Physics 53)* (Berlin: Springer) pp 217–60

[20] Chevrier J. Suck J-B, Capponi J J and Perroux M 1988 *Phys. Rev. Lett.* **61** 554–7
[21] Kolesnikov A I, Barkalov O I, Belash I T, Ponyatovsky E G, Lasjaunias J C, Buchenau U, Shober H R and Frick B 1993 *J. Phys.: Condens. Matter* **5** 4737–48
[22] Bellissent-Funel M-C, Teixeira J and Bosio L 1992 *Physics and Chemistry of Ice* ed N Maeno and T Hondoh (Sapporo: Hokkaido University Press) pp 98–102
[23] Whalley E, Klug D D, Floriano M A, Svensson E C and Sears V F 1987 *J. Physique Coll.* **48** C1 429–34